

On the Relationship Between RNN Hidden State Vectors and Semantic Ground Truth

Edi Muškardin^{1,2}, Martin Tappler^{2,1}, Ingo Pill¹,
Bernhard K. Aichernig², and Thomas Pock^{3,1}

¹ Silicon Austria Labs, TU Graz - SAL DES Lab, Graz, Austria

² Graz University of Technology, Institute of Software Technology, Graz, Austria

³ Graz University of Technology, Institute of Computer Graphics and Vision, Graz, Austria

Abstract. We examine the assumption that the hidden-state vectors of recurrent neural networks (RNNs) tend to form clusters of semantically similar vectors, which we dub the *clustering hypothesis*. While this hypothesis has been assumed in the analysis of RNNs in recent years, its validity has not been studied thoroughly on modern neural network architectures. We examine the clustering hypothesis in the context of RNNs that were trained to recognize regular languages. This enables us to draw on perfect ground-truth automata in our evaluation, against which we can compare the RNN’s accuracy and the distribution of the hidden-state vectors.

We start with examining the (piecewise linear) separability of an RNN’s hidden-state vectors into semantically different classes. We continue the analysis by computing clusters over the hidden-state vector space with multiple state-of-the-art unsupervised clustering approaches. We formally analyze the accuracy of computed clustering functions and the validity of the clustering hypothesis by determining whether clusters group semantically similar vectors to the same state in the ground-truth model. Our evaluation supports the validity of the clustering hypothesis in the majority of examined cases. We observed that the hidden-state vectors of well-trained RNNs are separable, and that the unsupervised clustering techniques succeed in finding clusters of similar state vectors.

Keywords: Recurrent Neural Networks · Clustering · Hidden-State Vectors · Linear Separability · Explainable AI · Finite-State Machines.

1 Introduction

In recent years we have seen significant advancements in the analysis and verification of artificial neural networks (ANNs) [18,13,31]. The motivation has been to establish trust in the growing landscape of machine-learned intelligent systems. Most of the work considered feed-forward ANNs that implement mathematical functions without internal states. In this work we shift the focus to recurrent neural networks (RNNs) that model processes with internal states. RNNs have

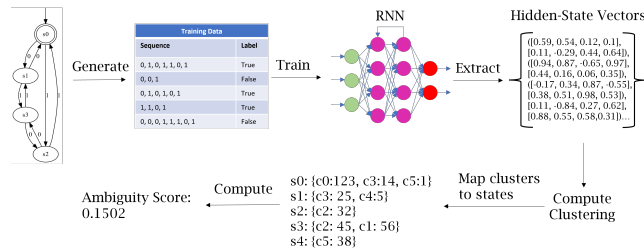


Fig. 1: Overview of the process for assessing the quality of clustering functions.

shown impressive results on high-dimensional data, like natural-language, but their internal decision-making progress is hard to interpret.

Consequently, many researchers have turned to the internals of RNNs in hopes of understanding the RNN decision-making process [27]. An important, yet scarcely examined, hypothesis in this field postulates that the hidden state vectors visited by a trained RNN while processing data form clusters. The states in a cluster are assumed to be semantically similar. For example, an RNN processing two semantically similar, but syntactically different natural-language sentences is assumed to traverse states that belong to the same state clusters.

Hence, the “*clustering hypothesis*” provides powerful analysis capabilities. It facilitates the creation of equivalence classes in the internal state space of RNNs by clustering. Put differently, it enables the discretization of RNN hidden state vectors to a finite number of equivalence classes. These classes enable further analyses, e.g., through the extraction of finite-state machines (FSMs) with states corresponding to clusters. Unlike RNNs, FSMs are well-understood and amenable to model-based reasoning. In recent years, the clustering hypothesis was the basis of several well received RNN analyses methods. For example, Dong et al. [9] relied on the clustering hypothesis to serve as an abstraction mechanism for models which enable identifications of adversarial attacks, while Michalenko et al. [24] learned functions from hidden states to (sets of) DFA states. While both approaches relied on some form of the clustering hypothesis, they also encountered, and subsequently coped with inaccuracies of computed clustering function. For example, [9] used probabilistic automata learning to minimize the error introduced by the computed clustering. While their approaches *might imply* the soundness of the clustering hypothesis, the validity of the hypothesis still remains questioned. For example, already in early work Kolen [20] warned against methods that rely on state-space discretization (clustering) due to the inherent information loss. Also, Zeng and Smyth [38] noticed problems with the clustering approach. In this paper, we return to this open question and thoroughly study the validity of the clustering hypothesis. The results of our empirical study shall increase the confidence in existing and future work on the validation and verification of RNNs.

More precisely, we investigate the following research questions: Are an RNN’s hidden-state vectors linearly separable (RQ1)? Is the clustering hypothesis assumed for RNNs valid (RQ2)? Do different training conditions affect clustering (RQ3)? We approach these questions by training RNNs on regular languages

with known minimal finite-state automata. By simulating the validation data on such RNNs we extract visited hidden states vectors, which are then used to compute multiple clustering functions. We analyze the correlation between derived clusters and automata states and assign an ambiguity score to each clustering configuration. Ideally, each cluster (or a set of clusters) should correspond to a unique state in the respective ground-truth automaton. An overview of this process can be seen at Fig. 1

The contributions of this work can be summarized as follows: (1) analyses of 1350 trained RNNs w.r.t. separability of their state space, (2) computation and analysis of clusters over the hidden-state vectors, (3) application of all methods on close-to-perfect RNNs, (4) and a framework containing all presented functionalities developed with AALPY [26], PyTorch [28], and scikit-learn [29]. To the best of our knowledge, this constitutes the first detailed empirical evaluation of the "clustering hypothesis".

Structure. In Sect. 2, we give preliminaries. Sect. 3 discusses our research questions in detail and presents techniques and accuracy metrics that we use in Sect. 4 for an empirical evaluation of the "clustering hypothesis". In Sect. 1 we discuss related work, and in Sect. 5 we draw conclusions and discuss future work.

Related Work. Omlin and Giles [27] were among the first to mine rules from RNNs. They proposed an algorithm for DFA extraction from a second-order RNN trained to recognize a regular language by applying a clustering algorithm over the RNN's hidden-state space. They also visually analyzed the clustering of the RNN states, postulating that they are well separated. Similar works can be found in [7,12,35]. Since then, RNN research made significant advancements and the clustering hypothesis was criticized [20].

Zeng and Smyth [38] observed that the "clustering hypothesis" [27] becomes unstable as longer sequences are used to extract hidden-state vectors. They propose changing the training as a solution. Schellhammer et al. [30] trained an Elman RNN on a natural language processing (NLP) task and constructed a state-transaction diagram representing a grammar of the data set with the help of clustering. However, they considered RNNs with only two hidden neurons. Wang et al. [34] empirically evaluated various conditions that might influence DFA extraction from second-order RNNs. Interestingly, they observed that rules extracted from RNNs were more precise than RNNs themselves in classifying longer sequences. Dong et al. [9] combined principles from passive stochastic automata learning, with abstraction achieved by clustering the hidden-state space of an RNN. Clustering enabled adversarial data detection via probabilistic verification. Hou and Zhou [17] extracted automata from different types of gated RNNs with the help of clustering. They also reason about the gating mechanism and its influence on the clustering. However, their evaluation is restricted to two regular languages and a coarse abstraction for an NLP task, where they limit the number of clusters to just two. We improve upon their analysis by considering a significantly larger number of study subjects, RNN types, clustering approaches, and parameterizations, thus providing more and nuanced insights into the clustering hypothesis. Michalenko et al. [24] examined the relationship

between hidden (Elman) RNN states and the states of DFAs used for training data generation. They learned decoding functions from hidden states to (sets of) DFA states and found that such (linear) functions exist, though some DFA states may need to be grouped. Their results suggest that “supervised clustering” may not enable perfect reconstruction of FSM rules, but rather non-deterministic approximations. In this paper, we examined *if unsupervised clustering enables reconstruction of the finite-state semantics of the concept that is learned*, thus taking a view that is closer to practice.

2 Preliminaries

Definition 1. *A deterministic finite automaton (DFA) over alphabet Σ is a tuple $A = (Q, q_0, \delta, F)$, where Q is a finite set of states, $q_0 \in Q$ is the initial state, $\delta : Q \times \Sigma \rightarrow Q$ is the transition function, $F \subseteq Q$ are the final states.*

A **deterministic finite automaton (DFA)** defines a regular language comprising its accepted words. We extend the transition function as usual to arbitrary-length sequences $s \in \Sigma^*$, i.e., $\delta(q, \epsilon) = q$ and $\delta(q, e \cdot s') = \delta(\delta(q, e), s')$, where ϵ is the empty sequence, $e \in \Sigma$, $s' \in \Sigma^*$. A word $w \in \Sigma^*$ is accepted iff $\delta(q_0, w) \in F$.

Moore machines extend DFA by producing an output from a discrete output alphabet O in every state defined by a function $\lambda : Q \rightarrow O$. We can view both DFAs and Moore machines as functions $m : \Sigma^* \rightarrow O$ with $m(w) = \lambda(\delta(q_0, w))$, where $\lambda(q) = q \in F$ for DFAs. A function m defines a classification problem on words, which has two classes in the case of *DFAs*. Note that a Moore machine defines a regular language over the alphabet $\Sigma \times O$. We train recurrent neural networks (RNNs) on such languages.

Recurrent neural networks (RNNs) model sequential processes and are trained on sequential data. By manipulating an internal state, which we call the hidden state in this paper, they capture temporal dependencies across several time steps. Based on the current hidden state, outputs are computed, which may be discrete in classification tasks or continuous in regression tasks. This makes them well-suited for applications, such as, natural language processing [5], intrusion detection [4], and time series forecasting in various domains. In this paper, we examine Elman RNNs [10], LSTMs [15], and GRUs [6]. Below we provide the definition of one-layer Elman RNNs following the PyTorch implementation [28], while definitions of other RNN types can be found in the appendix.

$$\begin{aligned} h_t &= g(x_t W_{ih}^T + b_{ih} + h_{t-1} W_{hh}^T + b_{hh}) \text{ where } g \in \{\tanh, \text{ReLU}\} \\ y_t &= f(h_t W_{ho}^T) \end{aligned}$$

Elman RNNs manipulate the hidden state h_t at time step t through a simple recurrent structure based on the previous hidden state h_{t-1} . The most common activation functions for the recurrent layer(s) are *tanh* and *rectified linear units* (ReLU). The current output y_t is computed through another neural network cell with an activation function f , which works analogously for LSTMs and GRUs. For classification, the softmax function is often used as activation. LSTMs

and GRUs improve upon Elman RNNs that suffer from the vanishing/exploding gradient problem, which makes long-term dependencies hard to infer [37].

We view an RNN as a pair of functions (r, o) , where $r : \mathbb{R}^h \times \mathbb{R}^m \rightarrow \mathbb{R}^h$ updates the hidden state based on the previous hidden state h_{t-1} and the current input i_t . We use a one-hot encoding for discrete inputs from an alphabet of size m . For simplicity, we also use this view for LSTMs by analyzing the state space spanned by the concatenation of the hidden state h_t and the cell state c_t of LSTMs. The output function $o : \mathbb{R}^h \rightarrow C$ maps the current hidden state to an output class in C . We train RNNs on sequences sampled from regular languages defined by DFAs and Moore machines. In the former case, we have $C = \{true, false\}$, where *true* denotes acceptance of the sequence processed so far. In the latter case, we have $C = O$, where O is an output alphabet and o maps to the last output produced by the corresponding Moore machine.

Multiclass Classification. We examine the correspondence between hidden state vectors and ground truth models represented by deterministic finite automata. Given a finite sample of vectors in \mathbb{R}^h labeled with corresponding automaton states from a set Q , we formulate a multiclass classification problem. We apply (generalized) linear models to solve the problem so that their accuracy provides insights about the (piecewise linear) separability of \mathbb{R}^h into decision regions corresponding to Q .

In this setting, we have a sample from $\mathcal{S} \subset \mathbb{R}^h \times Q$. A pair $(h, q) \in \mathcal{S}$, contains a vector h in the hidden state space of an RNN and an automaton state q , which is the class label for the classification problem. Our goal is to find a function $cl : \mathbb{R}^h \rightarrow Q$ that classifies vectors correctly. We apply two representative techniques for classification: linear discriminant analysis (LDA) and logistic regression (LR). Both techniques yield linear models, meaning that their output classes depend linearly on the hidden state vectors serving as inputs. LR is actually a generalized linear model since it uses a nonlinear transformation of the input space. However, for more information we refer to the literature [3].

Clustering. Clustering deals with the identification of structure in data, an important problem in unsupervised learning [22]. In contrast to multiclass classification, clustering techniques take unlabeled data points as inputs. Clustering groups data points into clusters, such that ideally data points in the same clusters are *similar* to each other and data points from different clusters shall be *dissimilar* from each other. The notion of similarity is generally a problem-specific measure. The input to a clustering technique is an unlabeled sample of data points \mathcal{US} , in our case: $\mathcal{US} \subset \mathbb{R}^h$. Thus, we can view a clustering as a function $c : \mathcal{US} \rightarrow K$ assigning cluster labels to data points. In this paper, we focus on popular, efficient techniques available in the library scikit-learn [29]. We apply k-means [21], a partitional clustering technique [22] and three density-based clustering techniques: mean shift [8], DBSCAN [11], and OPTICS [2].

K-means partitions data into k clusters, assigning each data point p to the cluster whose center is closest to p . The center is the mean of all data points in a cluster. K-means creates piecewise linear decision boundaries, where the distance from centers of a neighboring cluster is equal. Density-based techniques creates

Algorithm 1 Labeling of hidden states with automaton states.

Input: $A = \langle Q, q_0, \delta, F \rangle$, RNN (r, o) , initial hidden state h_0 , validation data $D_v \subset D$ Output: pairs of hidden and aut. states $\mathcal{H}\mathcal{Q}$ 1: $\mathcal{H}\mathcal{Q} \leftarrow \emptyset$ 2: for all $(w, label)$ in D_v do 3: $q \leftarrow q_0, hs \leftarrow h_0$	4: $\mathcal{H}\mathcal{Q} \leftarrow \mathcal{H}\mathcal{Q} \cup \{(hs, q)\}$ 5: for all i in w do 6: $q \leftarrow \delta(q, i)$ 7: $hs \leftarrow r(hs, \rho(i))$ ▷ ρ encodes inputs 8: $\mathcal{H}\mathcal{Q} \leftarrow \mathcal{H}\mathcal{Q} \cup \{(hs, q)\}$ 9: return $\mathcal{H}\mathcal{Q}$
---	--

clusters of arbitrary shape that are identified as regions with a high density of data points. **DBSCAN** defines regions as clusters if at least *minNeighbors* points are in a neighborhood of a size defined by a radius ϵ . By merging clusters that are close to each other, it finds arbitrarily-shaped clusters. **OPTICS** follows the same basic approach as DBSCAN, but improves it by mitigating the sensitivity on the neighborhood size ϵ [36]. Like k-means, **mean shift** clusters a dataset based on centroids. Conversely, however, it attempts to find maxima in the density function underlying the distribution of the data and does not require a preset number of clusters k . It uses a bandwidth parameter bw to define regions for the update of centroids. As k-means creates piecewise linear decision boundaries, it is the closest among the considered clustering techniques to LDA.

3 Method

This section presents the basis for the analysis of the “clustering hypothesis”. Firstly, we formulate our research questions and introduce the setting. Then, we provide details on the analysis including accuracy measures.

3.1 Research Questions

Setting. In our experiments, we train RNNs on regular languages over an alphabet Σ . For each regular language $L \subseteq \Sigma^*$, we sample a dataset $D \subset \Sigma^*$. We split the sample D into training data D_t and validation data D_v of sizes n_t and n_v . The former is solely used for training whereas the latter provides a stopping criterion for training and data for the analysis of the clustering hypothesis.

For the remainder of this section, we fix a regular language $L \subseteq \Sigma^*$ and a sample dataset $D \subset \Sigma^*$. Let $A = \langle Q, q_0, \delta, F \rangle$ be a minimal DFA accepting exactly L and let $R = (r, o)$ be an RNN over the hidden state space $H = \mathbb{R}^h$ trained to recognize L . By processing every word in D_v simultaneously with the recurrent part r of R and the minimal DFA A , we determine the hidden states traversed by R as well as the corresponding automaton states reached by A . We store these data as pairs $(h, q) \in H \times Q$. For the remainder of this section let $\mathcal{H}\mathcal{Q} \subset H \times Q$ be a concrete sample of such pairs and let \mathcal{H} be the same sample without states Q . Algorithm 1 formalizes the creation of $\mathcal{H}\mathcal{Q}$.

RQ1: Are an RNN’s hidden-state vectors linearly separable? As a first step, we investigate whether hidden-state vectors can be (piecewise linearly) separated into regions corresponding to automaton states. We formulate this

as a multiclass classification problem based on $\mathcal{H}\mathcal{Q}$, the sampled hidden-state vectors labeled by automaton states. That is, we train a classification model on $\mathcal{H}\mathcal{Q}$ to learn a function $cl : \mathbb{R}^h \rightarrow Q$ and we evaluate its accuracy at classifying hidden states correctly. We rely on (generalized) linear models LDA and LR for this task. This choice is motivated by the observation that non-linear functions were not required in a similar setting [24]. While *piecewise linear separability* and low classification error of linear models *do not imply that the hidden states form well-defined clusters*, we gain insights into the structure of the hidden-state space. For example, if piecewise linear separation is not possible then k-means will generally not find accurate clusters. Hence, by using linear models for separability we actually enable a fairer comparison to clustering.

RQ2: Is the clustering hypothesis assumed for RNNs valid? The main research question concerns the validity of the clustering hypothesis. To examine it experimentally, we consider two aspects related to the clustering of RNN states.

- **The definition of a cluster.** Works based on the hypothesis apply different clustering techniques, hence we will analyze the effect of different popular clustering techniques.
- **Usefulness of a cluster.** The appeal of clustering stems from its potential as an abstraction for RNNs, thus enabling model-based reasoning [9]. Hence, clusters should possess similar qualities as abstractions for software systems. Concrete hidden states *abstracted to the same clusters* should behave similarly. Moreover, an abstraction should be small enough to enable efficient subsequent analyses, thus we will examine the number of detected clusters.

We will analyze these aspects based on experiments with regular languages, where we know the minimal ground-truth automaton. Hence, answering **RQ2** in this context can also be formulated as: **Do hidden state clusters correlate with states of an automaton accepting the same language?**

RQ3: Do different training conditions affect clustering? RNN training parameters and initialization potentially affect clustering, therefore we investigate a different training initialization. We create RNNs from ground-truth automata as described below. These RNNs are guaranteed to form dense clusters. After introducing noise into the RNN weights, we will examine if training adjusts the weights in a way that again leads to well-formed, meaningful clusters.

3.2 RNN Construction

Our construction of RNNs to encode automata is similar to those proposed in [1,14,25], therefore we keep the presentation brief and provide the complete construction in the appendix. We use Elman RNNs with *tanh* activation and a single layer, which we use in the saturated area of *tanh*, where it works like a threshold gate. We implement δ of the ground-truth DFA by setting W_{ih} , W_{hh} , b_{ih} , and b_{hh} , and we implement $q \in F$ by setting output-layer weights W_{oh} .

An RNN encoding an automaton has a state space with dense clusters corresponding to transitions, i.e., such an RNN would form $|Q| \cdot |\Sigma|$ many clusters. Hence, we need to analyze whether RNNs learn such non-minimal representations. Attempting to further train such an RNN would usually stop immediately,

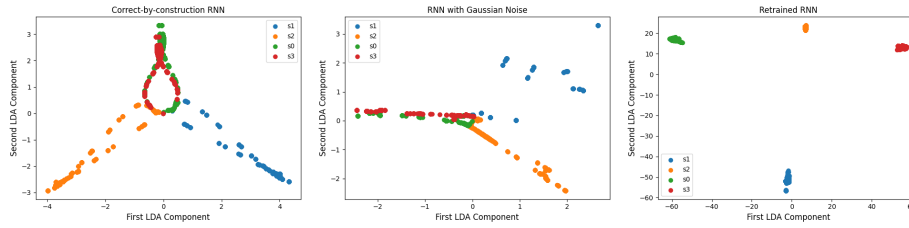


Fig. 2: Visualization of the hidden-state vectors of a correct-by-construction RNN(left), constructed RNN with Gaussian noise (middle), and trained noisy network (right), where we apply LDA for dimensionality reduction to 2D.

therefore we add noise to the weights W_{ih} , W_{hh} , b_{ih} , and b_{hh} to change the state transitions. This lets us analyze the effect of training *close-to-perfect* RNNs. We use Gaussian noise with a mean of 0 and a standard deviation of wn . Figure 2 shows a visualization of a constructed RNN, before and after introducing noise, and after training the noisy RNN. Here, we apply LDA for dimensionality reduction by projecting the data to a 2D-subspace that provides the best separation of data according to the LDA criterion.

3.3 Accuracy Metrics

We discuss the evaluation of the accuracy of RNNs and clusterings below. The former is based on the misclassification of words w.r.t. the ground-truth automaton A . Clustering accuracy is based on the ambiguity resulting from interpreting clusters as states of a finite-state model, compared to the states of A .

RNN Accuracy Validation. We validate the accuracy of an RNN $R = (r, o)$ by sampling words Σ^* to form an accuracy-validation set AV and checking whether R agrees with the ground-truth A , i.e., accepts the language L . For each word $w \in AV$ we process w with R by repeatedly applying r to get the final hidden state $h_{|w|}$ and computing the RNN output via $ro = o(h_{|w|})$. Then, we check whether ro agrees with the ground truth, where we define $agree_{R,L}(w) =_{def} ro \leftrightarrow w \in L$. We define the accuracy of R as $Acc_R(AV) = \frac{|\{agree_{R,L}(w) | w \in AV\}|}{|AV|}$.

Measuring the quality of clustering. We use the following intuition to define the optimality of clustering: *All data points in a cluster should correspond to a unique state in the ground truth A .* Formally, we can view a clustering as a function $c : \mathcal{H} \rightarrow K$ mapping sampled hidden states to cluster labels. This lets us compare a clustering c to the optimal mapping $hq : H \rightarrow Q$ based on the samples in $\mathcal{H}\mathcal{Q}$. To relate c and hq , we define the clustering of c as optimal if $hq = \alpha \circ c$ holds, where $\alpha : K \rightarrow Q$ renames cluster labels to states. Such a c allows extracting a DFA with states K from an RNN R that is equivalent to ground truth A if $Acc_R(AV) = 1$ and AV is large enough. To empirically evaluate a concrete c , we define the mismatch between c and hq based on entropy.

Before formally defining the mismatch between c and hq , which we term *ambiguity* of c , let us analyze criteria for good versus bad clusters. To apply clustering as an abstraction over H , a cluster should group semantically similar

states. Conversely, semantically different states should not be in the same cluster. Hence, we can derive that a clustering with $|K| < |Q|$ cannot be optimal, since all states in a minimal DFA are different, i.e., distinguishable through future behavior. In other words, a DFA extracted from the corresponding RNN with states identified by clusters K would not be equivalent to the ground-truth DFA A . If $|K| \geq |Q|$, the clustering may have a small mismatch, but the RNN may have learned a non-minimal representation if $|K| > |Q|$. The latter would not be desired for abstraction due to efficiency reasons. Next, we consider the best- and worst-case distributions of states in a cluster. Ideally, all hidden states in a cluster should map to the same automaton state. The worst case is achieved by a uniform distribution over states, as then the cluster would possess no semantic relation to the concept that has been learned.

We define ambiguity via the well-known concept of *information entropy*, which measures the degree of uncertainty (mismatch) in our clustering mappings. The entropy of our best-case clustering would be 0, while the worst-case clustering (uniform distribution) would give maximal entropy. Given, the general definition of entropy $Entropy(X) =_{def} -\sum_{x \in \mathcal{X}} p(x) \log p(x)$ with X being a random variable with outcomes in alphabet \mathcal{X} with distribution $p : \mathcal{X} \rightarrow [0, 1]$, we can instantiate it to measure the uncertainty in our cluster mappings via:

$$amb(k) = - \sum_{q \in Q} \frac{n_{q,k}}{n_k} \log_{|Q|} \frac{n_{q,k}}{n_k} \text{ where}$$

$$n_{q,k} = |\{(h, q) \mid (h, q) \in \mathcal{HQ}, c(h) = k\}| \text{ and } n_k = \sum_{q \in Q} n_{q,k}$$

$$amb(c) = \frac{\sum_{k \in K} amb(k)}{|K|} \quad wamb(c) = \frac{\sum_{k \in K} amb(k) \cdot n_k}{|\mathcal{HQ}|}$$

By using the logarithm with base $|Q|$ we ensure that the ambiguity is normalized to the interval $[0, 1]$. For the ambiguity of a clustering function, we compute the average of all clusters and the weighted average *wamb*. We noted above that ideally $hq = \alpha \circ c$ for a renaming α . This is achieved iff $amb(c) = 0$. We say that clustering is perfect if it achieves a (weighted) ambiguity of zero.

To enable a straightforward comparison between classification models and unsupervised clustering, we apply ambiguity also for classification models, by interpreting predicted classes as cluster labels. Note that ambiguity of zero coincides with a misclassification rate of zero. Thus, zero ambiguity of linear models implies (piecewise linear) separability on the sample dataset \mathcal{H} .

Alternatively to our notion of ambiguity, we could also use normalized mutual information (NMI), a commonly used estimate of clustering quality with an information-theoretic interpretation. However, clustering size affects NMI such that a perfect, but slightly non-minimal clustering may have a lower NMI than an ambiguous, but small clustering. Since the former (a perfect, non-minimal clusterings) is likely more useful for RNN analyses than the latter (imperfect clusterings), we focus on ambiguity and examine clustering size separately.

4 Evaluation

In this section, we present the experimental setup and results on the clustering hypothesis to answer the research questions defined in Sect. 3. The code required to reproduce all experiments can be found at ⁴.

4.1 Experimental Setup

Case Study Subjects. We performed experiments with 59 regular languages encoded by automata models. Five of the languages are evaluation subjects from the literature, including three of the Tomita grammars [33] (Tomita 3, 5, and 7), a Moore machine model of an MQTT server [32], and a regular expression used by Michalenko et al. [24]. Additionally, we randomly generated 30 DFAs and 24 Moore machines with up to 12 states and 72 transitions using AALPY [26].

Training. For each regular language, we trained an RNN to achieve perfect accuracy for 3 consecutive epochs on the validation data to potentially increase the likelihood of forming clusters in the hidden state space [23]. We trained Elman RNNs [10] with *tanh* and *ReLU*, LSTMs [16], and GRUs [6], each of them with one layer of size n , one layer of size $1.5n$, two layers of size n , where n is the number of transitions of the ground-truth automaton producing the language under consideration. We have chosen these network sizes, since a one-layer Elman RNN with n hidden neurons is sufficient to encode automata with n transitions, as in our RNN construction (see Sect. 3). Additionally, we also train slightly larger networks, as an increased size may be beneficial for training. We decided to not consider very large networks, as it would complicate the clustering analysis due to dimensionality reduction becoming more important, hindering us from concentrating on clustering approaches. For all experiments, we used the ADAM optimizer [19] with a learning rate of 0.0005. The training data consisted of $n_t = 50k$ randomly sampled words of lengths in the range $[1, 15]$, with labels derived from the ground-truth model. The validation data contained $n_v = 2000$ words, resulting in appr. $10k$ different hidden-state vectors for clustering. For all experiments, we trained two RNNs per configuration (network type, size).

Classification & Clustering. We used LDA and LR to learn classification models to determine whether automaton states can be separated in the hidden state space. Both approaches are supervised classification techniques, to which we provide $\mathcal{HS} \subset H \times Q$, sampled pairs of hidden states and automaton states.

For the clustering algorithms, we apply various parameterizations and use Euclidean distance as a distance metric. We set the k of k-means based on the size $n = |Q|$ of the minimal ground-truth automata A with $k \in \{n - 1, n, n + 1, 2n, 4n, 6n, 8n\}$. With the first three values, we check whether a good clustering exists that is close to the minimal automaton representation. We also use greater values because an RNN may learn a non-minimal representation, like in our construction. The evaluation languages have up to 6 symbols, thus $k = 6n$ would be sufficient for our construction of RNNs. We choose the parameters of

⁴ https://github.com/DES-Lab/Clustering_RNN_hidden_state_space

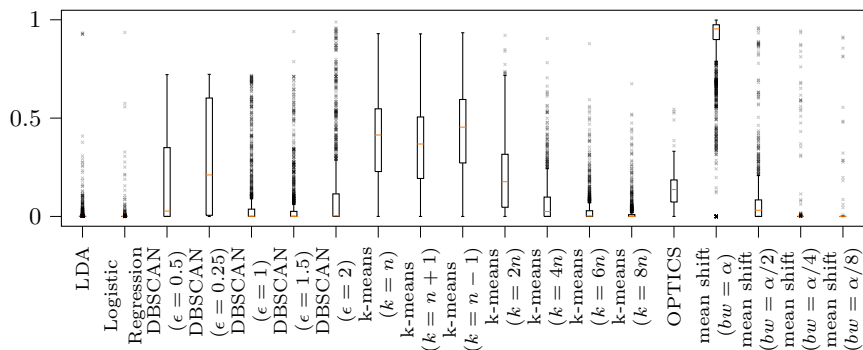


Fig. 3: Boxplots of the weighted ambiguity resulting from different clustering techniques for all 1350 experiments whose RNNs achieved at least 80% accuracy.

DBSCAN and *mean shift* as follows. For DBSCAN we experiment with multiples of the neighborhood size $\epsilon = 0.5$, the default in the scikit-learn library. We leave the other parameter *minNeighbors* at its default value of 5. For mean shift, we estimate the bandwidth *bw* with scikit-learn, which we denote α , to perform experiments with multiples of α . As OPTICS improves upon DBSCAN by mitigating its sensitivity on parameter values, we only apply its default parameterization. Since mean shift and OPTICS require more computation time than other techniques, we reduced the sample \mathcal{H} to 25% of its size for these two.

4.2 Overview of All Experiments

In the first set of experiments, we consider all four RNN types, Elman RNNs with ReLU and tanh activation functions, LSTMs, and GRU networks, as well as all clustering techniques. We evaluated all RNNs and only considered those whose accuracy ($agree_{R,L}$ from Sect. 3.3 evaluated on accuracy-validation data) was $\geq 80\%$. We chose this accuracy cutoff as, in practice, RNNs rarely achieve perfect generalization due to the complexity of the underlying task or quality of training data. In total, this resulted in a selection of 1350 from 1416 RNNs.

Figure 3 summarizes the results of these experiments. It shows boxplots of the weighted cluster ambiguity *wamb* resulting from different clustering techniques, with outliers denoted by small crosses. Furthermore, the second row of Table 1 shows the number of perfect clusterings, i.e. $wamb = 0$, achieved by each method.

We observe that the LDA and LR are able to achieve perfect classification in 74% and 91% of the cases, respectively. LDA has mean *wamb* of 0.0009 ± 0.05 , while LR’s mean was 0.0004 ± 0.039 . Relating to **RQ1**, this high level of accuracy indicates that in the majority of considered cases, even with networks that did not achieve perfect accuracy, *piecewise linear separability of the hidden state space is possible*. Below we will show that the level of accuracy increases for perfectly trained RNNs. Recall, however, that LDA and LR are derived using additional information about the correspondence between hidden and automaton

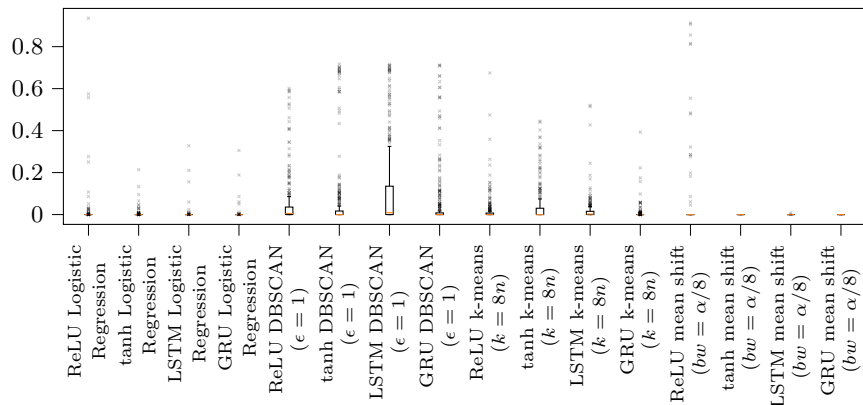


Fig. 4: Weighted ambiguity for selected methods sorted by network types.

states, which is usually not available, therefore we examine the ambiguity of unsupervised clustering approaches.

The median weighted ambiguity of DBSCAN with $\epsilon \geq 1$ is almost equal to 0, which means that in at least half of the cases, we can identify semantically meaningful discrete states from clusters. Likewise, k-means achieves a low ambiguity when given at least four times as many clusters as “necessary”, i.e., $k \geq 4n$. This means that RNNs seem to learn non-minimal representations of the concept that is being learned. OPTICS generally improves upon DBSCAN, but in this use case it seems to perform slightly worse than DBSCAN. The accuracy of clusters computed by mean shift depends on the parameterization of the bandwidth bw . The bandwidth estimated by scikit-learn results in a number of clusters that is smaller than n , causing high ambiguity. But as we decrease bw , in turn increasing the number of found clusters, mean shift becomes the best clustering method, even outperforming supervised classification approaches like LDA and LR. Regarding **RQ2**, we can state that *clusters correlate with automaton states*, with the caveat that proper parameterization is necessary.

Detailed results with mean and standard deviation, as well as maximum ambiguity and number of perfect clusterings of each approach are in the appendix.

4.3 Impact of Network Architecture

Next, we examine the influence of the RNN architecture on classification and clustering. Figure 4 shows the average weighted ambiguity achieved by LR and selected clustering parameterizations for each RNN architecture separately. GRU networks appear to create state space structures that lend themselves best to clustering with any of the approaches. Interestingly, Elman ReLU RNNs lead to the highest ambiguity on average, even for LR. A potential explanation is that ReLU activations are unbounded, whereas tanh, e.g., is bounded. Hence, tanh Elman RNNs may create clusters in the saturated area of tanh, as in our RNN encoding of automata. We conclude from these experiments that clustering techniques should be chosen in accordance with the RNN type under consideration.

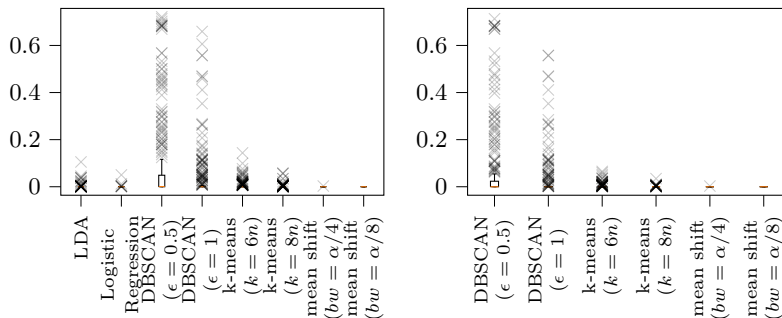


Fig. 5: Boxplots of the weighted ambiguity resulting from different clustering techniques for all 313 experiments with GRUs (left) and for a subset of 278 GRU experiments, where LDA and LR achieved perfect separability.

Clustering of GRU Networks. In the following, we examine the clustering hypothesis for GRU networks, for which we found particularly low ambiguity measurements. Figure 5 shows box plots of ambiguity values measured for different clustering techniques. On the left, we show measurements from all experiments involving GRUs and on the right, we show measurements from experiments, where LDA is able to perfectly separate hidden states corresponding to all automaton states.

We found that the hidden state space of the trained GRUs has a structure that is well-suited for linear separation of states. In 88% of the experiments, both LDA and LR can perfectly separate states.

This benefits k-means as well, which achieves lower ambiguity in all considered parameterizations when compared to other network types. In particular, k-means with $k = 8n$ performs very well, where the third quartile of the ambiguity values is equal to zero. From the other techniques, DBSCAN with $\epsilon = 1$ benefits from restricting the analysis to GRUs. OPTICS and especially mean shift are hardly affected. Focusing only on the experiments where LDA has an ambiguity of 0 (Fig. 5 (right)), we see that k-means performs especially well, with an ambiguity of at most 0.034 for $k = 8n$.

4.4 Training of Noisy Correct-by-Construction RNNs

The second set of experiments considers trained RNNs that have been initialized to the noisy “correct-by-construction” RNNs. That is, for each DFA we have computed an RNN with the method discussed in Sect. 3.2 and introduced Gaussian noise over the weights. The training was then performed on such an RNN initialized with noisy close-to-perfect weights. This set of experiments was performed on all DFAs, with a single RNN size and type, and three configurations of saturation and noise parameters. We considered only RNNs that achieved 100% accuracy, thus reducing this set of experiments to 95 RNNs.

The results can be seen in Fig. 6 and in the third row of Table 1. Both LDA and LR were able to perfectly classify hidden-state vectors in 92% and

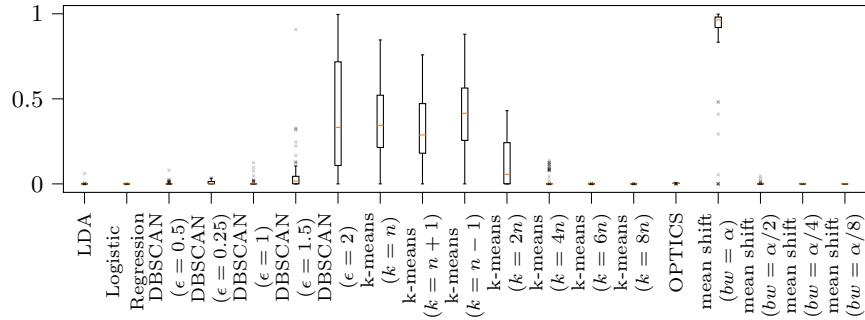


Fig. 6: Boxplots of the clustering ambiguity resulting from different clustering techniques from 95 trained noisy constructed RNNs.

Table 1: Number of perfect clustering (zero ambiguity) achieved by selected clustering method over both set of experiments.

Clustering Function	LDA	LR	DBSCAN			k-means			OPTICS	mean shift		
Parameters			0.5	0.25	1.5	n	$6n$	$8n$		$\alpha/2$	$\alpha/4$	$\alpha/8$
# Perfect Clustering (1350 experiments)	1003	1235	368	185	639	49	629	783	16	373	1296	1331
# Perfect Clustering (95 Experiments)	88	92	80	51	42	3	90	90	3	85	93	74

95% percent of the cases, respectively. DBSCAN managed to compute clusters with low ambiguity, but compared to the previous set of experiments, it achieved so with smaller ϵ . On average, OPTICS found clusters with very low ambiguity (0.003 ± 0.0008), but interestingly it found perfect clusterings in only 17% of the cases. K-means had similar performance as in the previous set of experiments, with $k = 6n$ and $k = 8n$ achieving near-perfect results. Once again, mean shift outperformed both LDA and LR, as well as other unsupervised clustering approaches. Concerning **RQ3**, we can state that *initial conditions do affect clustering*. For example, our constructed weights seem to lead to smaller distances in the state space, such that DBSCAN performed better with smaller ϵ .

4.5 Number of Clusters

We only considered ambiguity so far. As clustering is a tool for abstraction, we also need to look at the size of the abstraction, i.e., the number of clusters. K-means fixes this size, but the number of clusters derived by other approaches depends on their parameters *and* the given data. Figure 7 shows box plots of the number of clusters derived by different techniques for both previously discussed experiments. We show two instantiations of k-means as a reference.

We observe interesting trends between the two experiments. From Fig. 7, we can observe that the accuracy and initialization of an RNN has a large impact on the number of clusters. The right subplot of Fig. 7 shows that both DBSCAN parameterizations yield smaller numbers of clusters than k-means, but in the case where RNNs are not perfectly accurate ($\geq 80\%$) and are trained from scratch, DBSCAN finds substantially more clusters than k-means. The same

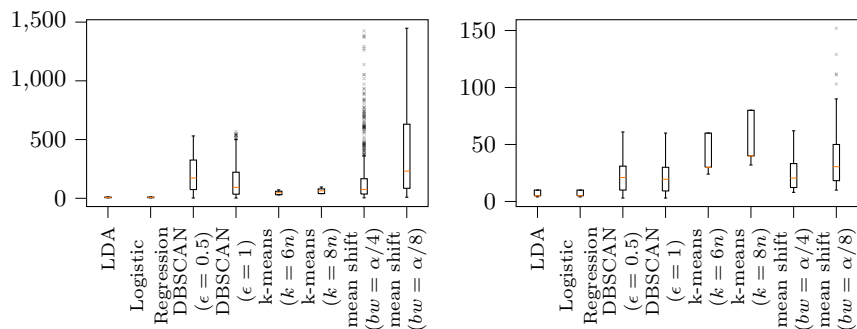


Fig. 7: Number of clusters found in experiments with RNNs trained from scratch (left) and with RNNs initialized with close-to-perfect weights (right).

trend, but with even bigger size differences can be observed for mean shift. These findings imply that while clustering functions with low ambiguity can be found for non-perfect RNNs, they tend to have more clusters than clustering functions computed on perfectly accurate RNNs. The fact that mean shift with $bw = \alpha/8$ finds up to $1.5k$ clusters in $\sim 2.5k$ data points (recall that we reduced the data for mean shift) and that the third quartile in Fig. 7 (left) is 500 weakens our findings regarding **RQ2**. The highly accurate clusterings found with mean shift hardly group states in many cases, thus making it trivial to achieve high accuracy. On average, most clustering approaches would improve the efficiency of model-based analysis of RNNs by reducing approximately $10k$ data points in the validation data to a few hundred clusters.

Discussion. Given our findings on the number of clusters, we should consider techniques and parameterizations that create reasonably-sized abstractions. K-means with $k = 8n$ achieves perfect clustering in 58% of the cases on RNNs trained from scratch (see Table 1). Additionally, we found that this k-means parameterization achieved a mean *wamb* of 0.018 overall, but in the most extreme case, *wamb* was 0.67. Hence, clusters mostly correlate with automaton states, if an appropriate clustering technique is applied. As such reasonably-sized clustering functions do not achieve high accuracy in some cases, we cannot rely on the clustering hypothesis alone in safety-critical applications, like autonomous driving. Additional techniques are needed to mitigate the error resulting from ambiguous clusters, like probabilistic automata learning [9]. To further validate the unambiguous (perfect) clustering functions, we extracted non-minimal automata from cluster labels, as described

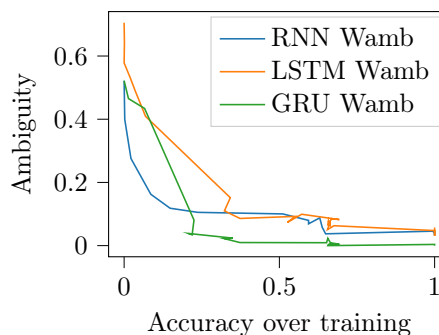


Fig. 8: Relationship between accuracy and ambiguity over the training process.

by Hou and Zhou [17]. Our findings conform to theirs: extracted non-minimal automata can be minimized to correspond to the ground-truth models.

Figure 8 shows the relationship between RNN accuracy and ambiguity over the training process. We observe that the ambiguity decreases during the training process, as the accuracy increases. This shows that the clustering hypothesis is related to RNN accuracy, and even further validates the ambiguity metric introduced in Sect. 3.3. In only few cases, accuracy decreases slightly as ambiguity decreases and vice versa, which explains the kinks in the graphs. However, there is generally a strong negative correlation, i.e., the more accurate an RNN gets, the clustering gets less ambiguous: the Spearman correlation coefficients are -0.87 , -0.96 , and -0.9 for Elman RNNs, LSTMs, and GRUs in Fig. 8. Additionally, if the RNN retains the accuracy over long sequences (100-200 input symbols), the clustering ambiguity remains constant.

5 Conclusion and Future Work

We revisited and formally analyzed the hypothesis that an RNN’s hidden-state vectors tend to form clusters. In our analysis, we examined the clustering hypothesis for RNNs that were trained to recognize regular languages. This provided us with a ground truth that allowed us to compare the identified clusters with the original finite-state semantics that underlie the learned concept. Additionally, we examined the (linear) separability of hidden-state vectors into regions corresponding to automata states.

In our experiments, we observed that the **hidden-state vectors can be (piecewise linearly) separated** in most of the considered cases. This finding indicates that it is potentially possible to derive meaningful mappings from hidden-state vectors to automata states. Considering unsupervised clustering, the regions identified by classifiers may contain multiple clusters and clusters may span across decision boundaries. However, we show that it is **possible to compute clustering functions that correlate with automata states**. For example, clusterings obtained by k-means with large k overall achieved high accuracy and perfect accuracy in 58% of our experiments. Furthermore, in cases of perfect clustering, we observed that RNNs learn non-minimal representations of the regular languages on which they were trained. The selection of a clustering method and its parameterization greatly affects the clustering accuracy, hindering the possibility of using an out-of-the-box clustering algorithm as a means of RNN hidden-state space abstraction.

We identify various avenues for future work. With RNN verification being our ultimate goal, we will investigate ways to mitigate imprecisions and errors resulting from imperfect clustering. A stochastic interpretation of RNNs and stochastic automata learning over clusters seems promising [9]. Further analysis of factors affecting the clustering is important as well, examples being the effect of different optimizers or overtraining. Finally, we will investigate how to adapt the training and architecture of RNNs such that clusters are likely to form, which would enable explainability-by-design.

Acknowledgements. This work has been supported by the "University SAL Labs" initiative of Silicon Austria Labs (SAL) and its Austrian partner universities for applied fundamental research for electronic based systems.

References

1. Alquézar, R., Sanfeliu, A.: An algebraic framework to represent finite state machines in single-layer recurrent neural networks. *Neural Comput.* **7**(5), 931–949 (1995). <https://doi.org/10.1162/neco.1995.7.5.931>, <https://doi.org/10.1162/neco.1995.7.5.931>
2. Ankerst, M., Breunig, M.M., Kriegel, H., Sander, J.: OPTICS: ordering points to identify the clustering structure. In: Delis, A., Faloutsos, C., Ghandeharizadeh, S. (eds.) SIGMOD 1999, Proceedings ACM SIGMOD International Conference on Management of Data, June 1-3, 1999, Philadelphia, Pennsylvania, USA. pp. 49–60. ACM Press (1999). <https://doi.org/10.1145/304182.304187>, <https://doi.org/10.1145/304182.304187>
3. Bishop, C.M.: Pattern recognition and machine learning, 5th Edition. Information science and statistics, Springer (2007), <https://www.worldcat.org/oclc/71008143>
4. Bontemps, L., Cao, V.L., McDermott, J., Le-Khac, N.: Collective anomaly detection based on long short-term memory recurrent neural networks. In: Dang, T.K., Wagner, R.R., Küng, J., Thoai, N., Takizawa, M., Neuhold, E.J. (eds.) Future Data and Security Engineering - Third International Conference, FDSE 2016, Can Tho City, Vietnam, November 23-25, 2016, Proceedings. Lecture Notes in Computer Science, vol. 10018, pp. 141–152 (2016). https://doi.org/10.1007/978-3-319-48057-2_9, https://doi.org/10.1007/978-3-319-48057-2_9
5. Cheng, J., Dong, L., Lapata, M.: Long short-term memory-networks for machine reading. In: Su, J., Carreras, X., Duh, K. (eds.) Proceedings of the 2016 Conference on Empirical Methods in Natural Language Processing, EMNLP 2016, Austin, Texas, USA, November 1-4, 2016. pp. 551–561. The Association for Computational Linguistics (2016). <https://doi.org/10.18653/v1/d16-1053>, <https://doi.org/10.18653/v1/d16-1053>
6. Cho, K., van Merriënboer, B., Bahdanau, D., Bengio, Y.: On the properties of neural machine translation: Encoder-decoder approaches. *CoRR* **abs/1409.1259** (2014), <http://arxiv.org/abs/1409.1259>
7. Cleeremans, A., Servan-Schreiber, D., McClelland, J.L.: Finite state automata and simple recurrent networks. *Neural Comput.* **1**(3), 372–381 (1989). <https://doi.org/10.1162/neco.1989.1.3.372>, <https://doi.org/10.1162/neco.1989.1.3.372>
8. Comaniciu, D., Meer, P.: Mean shift: A robust approach toward feature space analysis. *IEEE Trans. Pattern Anal. Mach. Intell.* **24**(5), 603–619 (2002). <https://doi.org/10.1109/34.1000236>, <https://doi.org/10.1109/34.1000236>
9. Dong, G., Wang, J., Sun, J., Zhang, Y., Wang, X., Dai, T., Dong, J.S., Wang, X.: Towards interpreting recurrent neural networks through probabilistic abstraction. In: 35th IEEE/ACM International Conference on Automated Software Engineering, ASE 2020, Melbourne, Australia, September 21-25, 2020. pp. 499–510. IEEE (2020). <https://doi.org/10.1145/3324884.3416592>, <https://doi.org/10.1145/3324884.3416592>
10. Elman, J.L.: Finding structure in time. *Cogn. Sci.* **14**(2), 179–211 (1990). https://doi.org/10.1207/s15516709cog1402_1, https://doi.org/10.1207/s15516709cog1402_1

11. Ester, M., Kriegel, H., Sander, J., Xu, X.: A density-based algorithm for discovering clusters in large spatial databases with noise. In: Simoudis, E., Han, J., Fayyad, U.M. (eds.) Proceedings of the Second International Conference on Knowledge Discovery and Data Mining (KDD-96), Portland, Oregon, USA. pp. 226–231. AAAI Press (1996), <http://www.aaai.org/Library/KDD/1996/kdd96-037.php>
12. Giles, C.L., Miller, C.B., Chen, D., Sun, G., Chen, H., Lee, Y.: Extracting and learning an unknown grammar with recurrent neural networks. In: Moody, J.E., Hanson, S.J., Lippmann, R. (eds.) Advances in Neural Information Processing Systems 4, [NIPS Conference, Denver, Colorado, USA, December 2-5, 1991]. pp. 317–324. Morgan Kaufmann (1991), <http://papers.nips.cc/paper/555-extracting-and-learning-an-unknown-grammar-with-recurrent-neural-networks>
13. Gopinath, D., Katz, G., Pasareanu, C.S., Barrett, C.W.: Deepsafe: A data-driven approach for checking adversarial robustness in neural networks. CoRR **abs/1710.00486** (2017), <http://arxiv.org/abs/1710.00486>
14. Goudreau, M.W., Giles, C.L., Chakradhar, S.T., Chen, D.: First-order versus second-order single-layer recurrent neural networks. IEEE Trans. Neural Networks **5**(3), 511–513 (1994). <https://doi.org/10.1109/72.286928>, <https://doi.org/10.1109/72.286928>
15. Hochreiter, S., Schmidhuber, J.: Long short-term memory. Neural Comput. **9**(8), 1735–1780 (1997). <https://doi.org/10.1162/neco.1997.9.8.1735>, <https://doi.org/10.1162/neco.1997.9.8.1735>
16. Hochreiter, S., Schmidhuber, J.: Long short-term memory. Neural Comput. **9**(8), 1735–1780 (1997). <https://doi.org/10.1162/neco.1997.9.8.1735>, <https://doi.org/10.1162/neco.1997.9.8.1735>
17. Hou, B., Zhou, Z.: Learning with interpretable structure from gated RNN. IEEE Trans. Neural Networks Learn. Syst. **31**(7), 2267–2279 (2020). <https://doi.org/10.1109/TNNLS.2020.2967051>, <https://doi.org/10.1109/TNNLS.2020.2967051>
18. Huang, X., Kwiatkowska, M., Wang, S., Wu, M.: Safety verification of deep neural networks. In: Majumdar, R., Kuncak, V. (eds.) Computer Aided Verification - 29th International Conference, CAV 2017, Heidelberg, Germany, July 24-28, 2017, Proceedings, Part I. Lecture Notes in Computer Science, vol. 10426, pp. 3–29. Springer (2017). https://doi.org/10.1007/978-3-319-63387-9_1, https://doi.org/10.1007/978-3-319-63387-9_1
19. Kingma, D.P., Ba, J.: Adam: A method for stochastic optimization. In: Bengio, Y., LeCun, Y. (eds.) 3rd International Conference on Learning Representations, ICLR 2015, San Diego, CA, USA, May 7-9, 2015, Conference Track Proceedings (2015), <http://arxiv.org/abs/1412.6980>
20. Kolen, J.F.: Fool’s gold: Extracting finite state machines from recurrent network dynamics. In: Cowan, J.D., Tesauro, G., Alspector, J. (eds.) Advances in Neural Information Processing Systems 6, [7th NIPS Conference, Denver, Colorado, USA, 1993]. pp. 501–508. Morgan Kaufmann (1993), <http://papers.nips.cc/paper/757-fools-gold-extracting-finite-state-machines-from-recurrent-network-dynamics>
21. MacQueen, J.B.: Some methods for classification and analysis of multivariate observations. In: Cam, L.M.L., Neyman, J. (eds.) Proc. of the fifth Berkeley Symposium on Mathematical Statistics and Probability. vol. 1, pp. 281–297. University of California Press (1967)
22. Madhulatha, T.S.: An overview on clustering methods. CoRR **abs/1205.1117** (2012), <http://arxiv.org/abs/1205.1117>
23. Merrill, W., Tsilivis, N.: Extracting finite automata from rnns using state merging. CoRR **abs/2201.12451** (2022), <https://arxiv.org/abs/2201.12451>

24. Michalenko, J.J., Shah, A., Verma, A., Baraniuk, R.G., Chaudhuri, S., Patel, A.B.: Representing formal languages: A comparison between finite automata and recurrent neural networks. In: 7th International Conference on Learning Representations, ICLR 2019, New Orleans, LA, USA, May 6-9, 2019. OpenReview.net (2019), <https://openreview.net/forum?id=H1zeHnA9KX>
25. Minsky, M.L.: Computation: Finite and Infinite Machines. Prentice-Hall, Inc., USA (1967)
26. Muškardin, E., Aichernig, B., Pill, I., Pferscher, A., Tappler, M.: Aalpy: an active automata learning library. *Innovations in Systems and Software Engineering* pp. 1–10 (03 2022). <https://doi.org/10.1007/s11334-022-00449-3>
27. Omlin, C.W., Giles, C.L.: Extraction of rules from discrete-time recurrent neural networks. *Neural Networks* **9**(1), 41–52 (1996). [https://doi.org/10.1016/0893-6080\(95\)00086-0](https://doi.org/10.1016/0893-6080(95)00086-0), [https://doi.org/10.1016/0893-6080\(95\)00086-0](https://doi.org/10.1016/0893-6080(95)00086-0)
28. Paszke, A., Gross, S., Massa, F., Lerer, A., Bradbury, J., Chanan, G., Killeen, T., Lin, Z., Gimelshein, N., Antiga, L., Desmaison, A., Kopf, A., Yang, E., DeVito, Z., Raison, M., Tejani, A., Chilamkurthy, S., Steiner, B., Fang, L., Bai, J., Chintala, S.: Pytorch: An imperative style, high-performance deep learning library. In: Wallach, H., Larochelle, H., Beygelzimer, A., d'Alché-Buc, F., Fox, E., Garnett, R. (eds.) *Advances in Neural Information Processing Systems* 32, pp. 8024–8035. Curran Associates, Inc. (2019), <http://papers.neurips.cc/paper/9015-pytorch-an-imperative-style-high-performance-deep-learning-library.pdf>
29. Pedregosa, F., Varoquaux, G., Gramfort, A., Michel, V., Thirion, B., Grisel, O., Blondel, M., Prettenhofer, P., Weiss, R., Dubourg, V., Vanderplas, J., Passos, A., Cournapeau, D., Brucher, M., Perrot, M., Duchesnay, E.: Scikit-learn: Machine learning in Python. *Journal of Machine Learning Research* **12**, 2825–2830 (2011)
30. Schellhammer, I., Diederich, J., Towsey, M., Brugman, C.: Knowledge extraction and recurrent neural networks: An analysis of an elman network trained on a natural language learning task. In: Powers, D.M.W. (ed.) *Proceedings of the Joint Conference on New Methods in Language Processing and Computational Natural Language Learning, NeMLaP/CoNLL 1998*, Macquarie University, Sydney, NSW, Australia, January 11-17, 1998. pp. 73–78. ACL (1998), <https://aclanthology.org/W98-1209/>
31. Sun, Y., Wu, M., Ruan, W., Huang, X., Kwiatkowska, M., Kroening, D.: Concolic testing for deep neural networks. In: Huchard, M., Kästner, C., Fraser, G. (eds.) *Proceedings of the 33rd ACM/IEEE International Conference on Automated Software Engineering, ASE 2018*, Montpellier, France, September 3-7, 2018. pp. 109–119. ACM (2018). <https://doi.org/10.1145/3238147.3238172>, <https://doi.org/10.1145/3238147.3238172>
32. Tappler, M., Aichernig, B.K., Bloem, R.: Model-based testing IoT communication via active automata learning. In: 2017 IEEE International Conference on Software Testing, Verification and Validation, ICST 2017, Tokyo, Japan, March 13-17, 2017. pp. 276–287. IEEE Computer Society (2017). <https://doi.org/10.1109/ICST.2017.32>, <https://doi.org/10.1109/ICST.2017.32>
33. Tomita, M.: Dynamic construction of finite automata from examples using hill-climbing. In: *Conference of the Cognitive Science Society*. pp. 105–108 (1982)
34. Wang, Q., Zhang, K., II, A.G.O., Xing, X., Liu, X., Giles, C.L.: An empirical evaluation of rule extraction from recurrent neural networks. *Neural Comput.* **30**(9) (2018). https://doi.org/10.1162/neco_a_01111, https://doi.org/10.1162/neco_a_01111

35. Watrous, R.L., Kuhn, G.M.: Induction of finite-state automata using second-order recurrent networks. In: Moody, J.E., Hanson, S.J., Lippmann, R. (eds.) *Advances in Neural Information Processing Systems* 4, [NIPS Conference, Denver, Colorado, USA, December 2-5, 1991]. pp. 309–317. Morgan Kaufmann (1991), <http://papers.nips.cc/paper/560-induction-of-finite-state-automata-using-second-order-recurrent-networks>
36. Xu, D., Tian, Y.: A comprehensive survey of clustering algorithms. *Annals of Data Science* **2** (08 2015). <https://doi.org/10.1007/s40745-015-0040-1>
37. Zachary Chase Lipton, John Berkowitz, C.E.: A critical review of recurrent neural networks for sequence learning. *CoRR* **abs/1506.00019** (2015), <http://arxiv.org/abs/1506.00019>
38. Zeng, Z., Goodman, R.M., Smyth, P.: Learning finite state machines with self-clustering recurrent networks. *Neural Comput.* **5**(6), 976–990 (1993). <https://doi.org/10.1162/neco.1993.5.6.976>, <https://doi.org/10.1162/neco.1993.5.6.976>

A Appendix

A.1 Appendix A – RNNs.

Mathematical definitions of RNNs. Below, we provide the mathematical definitions of LSTMs and GRUs following the PyTorch implementation [28].

LSTMs:

$$\begin{aligned}
 i_t &= \sigma(W_{ii}x_t + b_{ii} + W_{hi}h_{(t-1)} + b_{hi}) \\
 f_t &= \sigma(W_{if}x_t + b_{if} + W_{hf}h_{(t-1)} + b_{hf}) \\
 g_t &= \tanh(W_{ig}x_t + b_{ig} + r_t * (W_{hg}h_{(t-1)} + b_{hg})) \\
 o_t &= \sigma(W_{io}x_t + b_{io} + W_{ho}h_{(t-1)} + b_{ho}) \\
 c_t &= f_t \odot c_{(t-1)} + i_t \odot g_t \text{ where } \odot \text{ is the Hadamard product and} \\
 &\quad \sigma \text{ is the sigmoid function} \\
 h_t &= o_t \odot \tanh(c_t)
 \end{aligned}$$

GRUs:

$$\begin{aligned}
 r_t &= \sigma(W_{ir}x_t + b_{ir} + W_{hr}h_{(t-1)} + b_{hr}) \\
 z_t &= \sigma(W_{iz}x_t + b_{iz} + W_{hz}h_{(t-1)} + b_{hz}) \\
 n_t &= \tanh(W_{in}x_t + b_{in} + r_t \odot (W_{hn}h_{(t-1)} + b_{hn})) \\
 h_t &= (1 - z_t) \odot n_t + z_t \odot h_{(t-1)}
 \end{aligned}$$

Automata Encoding via RNNs. In the following, we provide a more detailed presentation of the RNN-based automata encoding. Recall that we use Elman RNNs with tanh activation and a single layer to encode automata. Similar encodings have been proposed in [1,14,25].

Our RNN-encoding of an automaton operates on one-hot encoded transitions of the ground-truth DFA A . We encode transitions rather than states, because one-layer first-order RNNs cannot encode all DFAs when they are restricted to one-hot encoded states [14]. Thus, we have for the hidden state space size $h = |Q| \cdot |\Sigma|$ and we impose a fixed ordering on the states Q and the alphabet Σ . Let $t_{i,j} = (q_i, e_j)$ be the transition labeled e_j originating in state q_i . We denote its encoding $\pi(q_i, e_j)$, which is a vector in \mathbb{R}^h , where exactly one element equals 1 and all others are -1 . The element set to 1 is at the position $i + (j \cdot |Q|)$. Let $\psi(q_i)$ be the encoding of the i^{th} state, a vector in \mathbb{R}^h , which is 1 at indexes $i + j \cdot |Q|$ for $j \in \{1, \dots, |\Sigma|\}$ and -1 otherwise. This encoding only shows up as a temporary value in the construction. Furthermore, let $\rho(e_j)$ be the one-hot encoding of a symbol e_j , a vector in $\mathbb{R}^{|\Sigma|}$ where exactly one element is equal to 1 and all others are 0. The basic idea is to set the weights of an RNN (r, o) so that r always operates in the saturated area of tanh, making tanh work like a binary threshold gate. For this reason, π and ψ use 1 and -1 (limits of tanh).

At time step t , the function r maps the previous transition $\pi(q_{t-1}, e_{t-1})$ and the new input $\rho(e_t)$ to the encoding of the next transition $\pi(\delta(q_{t-1}, e_{t-1}), e_t)$, where δ is the transition function of the DFA. To encode the whole DFA, we first set the RNN weights W_{hh} such that it maps an encoded transition to its encoded target state. Hence, for each transition (q_i, e_j) , we need to ensure that $W_{hh}\pi(q_i, e_j) \approx \psi(\delta(q_i, e_j))$, where $\delta(q_i, e_j)$ is the target state. As we apply \tanh as activation, we formulate this as $W_{hh}\pi(q_i, e_j) \geq \psi(\delta(q_i, e_j))H_r$, where H_r is a scalar factor defining how far we go into saturation. This factor ensures that we use \tanh in a region, where it maps to values close to -1 and 1 . For each of the $|Q| \cdot |\Sigma|$ transitions, we have a system of $h = |Q| \cdot |\Sigma|$ linear inequations. Hence, we have h^2 inequations and h^2 weights in the square matrix W_{hh} that we can adjust. By considering that all transition encodings are unique, it is easy to show that the complete system of inequations always has a solution.

To map an encoded state and encoded input to an encoded transition, we set the remaining weights as follows:

$$W_{ih} = (wih)_{i=1, \dots, |Q| \cdot |\Sigma|; j=1, \dots, |\Sigma|}, \text{ where } wih = \begin{cases} 0 & \text{if } [i/|\Sigma|] = j \\ -H_r & \text{otherwise} \end{cases}$$

$$b_{ih} = \mathbf{1} \cdot (-0.5) \cdot H_r \text{ and } b_{hh} = \mathbf{0}$$

where $\mathbf{1}$ and $\mathbf{0}$ are vectors containing 1 and 0

The matrix W_{ih} “selects” one part of the state encoding computed by $h' = W_{hh}\pi(q_i, e_j)$ via adding $W_{ih}x_t$ to h' , where $\rho(e_t) = x_t$ is the encoded input at time step t . This addition makes the intermediate vector $W_{hh}\pi(q_i, e_j) + W_{ih}x_t$ negative everywhere except at the indexes corresponding to the current input.

Additionally adding the bias term b_{hh} ensures that the final vector computed before applying \tanh is in a proper range and negative everywhere except at exactly one index. This term and the weights in W_{ih} are multiplied by the saturation factor H_r , such that after applying \tanh , we get approximately the encoding of a transition.

For the output layer, we create a $2 \times h$ matrix W_{oh} following a similar approach as for W_{hh} . Let τ be the one-hot encoding of *true* and *false*. We require for each transition (q_i, e_j) that $\sigma(W_{oh}\pi(q_i, e_j)) = \tau(\delta(q_i, e_j) \in F)$, as we use the sigmoid function σ as activation. In order to use σ in saturation, we again use a saturation factor H_o and formulate this as an inequality $W_{oh}\pi(q_i, e_j) \geq H_o\tau(\delta(q_i, e_j) \in F)$. Finally, we solve a linear inequation system of $2 \cdot |Q| \cdot |\Sigma|$ inequations to compute W_{oh} .

Training an RNN with weights computed as described above would yield a perfect RNN, where the state space would form dense clusters. However, there would be $|Q| \cdot |\Sigma|$ many clusters, so we need to analyze whether RNNs learn such non-minimal representations. Moreover, attempting to further train such an RNN would usually stop immediately. For this reason, we add noise to the weights W_{ih} , W_{hh} , b_{ih} , and b_{hh} to change the state transitions, so that we can analyze the effect of training *close-to-perfect* RNNs. We use Gaussian noise with a mean of 0 and standard deviation of wn .

A.2 Appendix B – Additional Evaluation Details

In the following, we provide additional details on the experimental setup and additional experimental results in tables.

Case Study Subjects. We used regular language from the literature including three of the Tomita grammars [33], where we have chosen Tomita 3, 5, and 7, as they define the most interesting languages. For example, Tomita 5 defines a parity language, which are difficult to learn for RNNs [14]. The Tomita grammars have five, four, and four states, respectively, and an alphabet of size two. The MQTT server that we used in the evaluation has seven states, six inputs, and six outputs, and the regular expression from Michaelenko et al. [24] has seven states and an alphabet containing four symbols.

The randomly generated DFAs have five or ten states, and alphabet sizes of two, four, or six. For each combination of state and alphabet size, we generated five DFAs. We generated three Moore machines for each combination of eight and twelve states, two and four inputs, and three and five outputs. Note that Moore machines encode regular languages that contain all possible input-output sequences. From an RNN perspective, they enable us to analyze how multi-class classification tasks affect clustering.

As noted in Sect. 4, we constructed RNNs to encode each of the DFAs. We applied the following parameters for saturation and noise in the construction of these close-to-perfect RNNs:

- $H_r = 1.5, H_o = 1.5, wn = 0.05$
- $H_r = 2, H_o = 2, wn = 0.1$
- $H_r = 3, H_o = 3, wn = 0.2$

Additional Results. In Table 2 and Table 3, we show detailed results from our clustering experiments performed on RNNs trained from scratch and on RNNs initialized with close-to-perfect weights, respectively. The tables show similar trends as the figures in the main part of the paper, but provide more details.

Extraction of cluster automata. Figure 9 depicts a non-minimal automaton extracted from an RNN trained on the Tomita 5 grammar. The extracted model is a non-minimal representation of the ground truth model, which is shown on the left-hand side of Fig. 1. We have applied the extraction method found in [17] with multiple clustering functions that achieved perfect accuracy, where Fig. 9 is based on k-means clustering with $k = 4n$. Basically, we create one DFA state for each cluster $k \in K$. For the transitions, suppose that (h, q) and (h', q') are pairs of hidden states and automaton states collected consecutively while processing symbol e . In this case, we add a transitions from $c(h)$ to $c(h')$ labeled by e , where c is the clustering function. If the RNN outputs *true* for one hidden state in a cluster k , we add k to the accepting states. While the extracted model size varied, all extracted automata were non-minimal representations of the ground-truth model that was used to train the RNN. Our findings conform

Table 2: Clustering ambiguity results from 1350 RNN’s that achieved 80% accuracy.

Clustering Function	Ambiguity		Weighted Ambiguity		Number of Clusters		# Perfect Clustering
	Mean \pm Std Dev	Max	Mean \pm Std Dev	Max	Mean \pm Std Dev	Max	
LDA	0.01 \pm 0.06	0.933	0.009 \pm 0.05	0.933	8 \pm 2.5	15	1003
Logistic Regression	0.003 \pm 0.036	0.935	0.004 \pm 0.039	0.935	8 \pm 2.5	12	1235
DBSCAN ($\epsilon = 0.5$)	0.002 \pm 0.002	0.025	0.179 \pm 0.239	0.721	200 \pm 140	531	368
DBSCAN ($\epsilon = 0.25$)	0.003 \pm 0.002	0.02	0.29 \pm 0.276	0.772	210 \pm 118	506	185
DBSCAN ($\epsilon = 1$)	0.005 \pm 0.025	0.672	0.066 \pm 0.15	0.716	143 \pm 135	568	591
DBSCAN ($\epsilon = 1.5$)	0.016 \pm 0.063	0.939	0.05 \pm 0.123	0.939	99 \pm 115	596	639
DBSCAN ($\epsilon = 2$)	0.057 \pm 0.144	0.989	0.110 \pm 0.208	0.98	69 \pm 90	560	514
k-means ($k = n$)	0.359 \pm 0.199	0.863	0.395 \pm 0.207	0.929	8.5 \pm 2.5	12	49
k-means ($k = n + 1$)	0.322 \pm 0.131	0.811	0.356 \pm 0.201	0.928	9.5 \pm 2.5	13	68
k-means ($k = n - 1$)	0.401 \pm 0.2	0.895	0.428 \pm 0.21	0.934	7.5 - 2.5	11	42
k-means ($k = 2n$)	0.175 \pm 0.154	0.736	0.2 \pm 0.172	0.92	16 \pm 5	24	209
k-means ($k = 4n$)	0.06 \pm 0.091	0.652	0.068 \pm 0.105	0.904	33 \pm 10	48	432
k-means ($k = 6n$)	0.0291 \pm 0.065	0.585	0.032 \pm 0.075	0.878	50 \pm 15	72	629
k-means ($k = 8n$)	0.017 \pm 0.051	0.54	0.0181 \pm 0.057	0.674	67 \pm 21	96	783
OPTICS	0.006 \pm 0.003	0.06	0.134 \pm 0.071	0.544	156 \pm 20	206	16
mean shift ($bw = \alpha$)	0.847 \pm 0.244	0.998	0.878 \pm 0.201	0.998	1.35 \pm 1.2	20	84
mean shift ($bw = \alpha/2$)	0.038 \pm 0.063	0.935	0.073 \pm 0.136	0.958	37 \pm 51	829	373
mean shift ($bw = \alpha/4$)	0.001 \pm 0.014	0.246	0.011 \pm 0.086	0.943	136 \pm 178	1425	1296
mean shift ($bw = \alpha/8$)	0.0004 \pm 0.005	0.09	0.005 \pm 0.06	0.912	391 \pm 397	1448	1331

Table 3: Results from 94 RNNs that were trained to 100% accuracy after introducing noise to “correct-by-construction” RNN.

Clustering Function	Ambiguity		Weighted Ambiguity		Number of Clusters		# Perfect Clustering
	Mean \pm Std Dev	Max	Mean \pm Std Dev	Max	Mean \pm Std Dev	Max	
LDA	0.0007 \pm 0.006	0.06	0.0004 \pm 0.004	0.039	7 \pm 2.5	10	88
Logistic Regression	8.22e-06 \pm 5.8e-05	0.0005	9.01e-06 \pm 6.3e-05	0.0005	7 \pm 2.5	10	92
DBSCAN ($\epsilon = 0.5$)	0.002 \pm 0.009	0.07	0.001 \pm 0.014	0.14	24.5 \pm 15.8	61	80
DBSCAN ($\epsilon = 0.25$)	0.007 \pm 0.009	0.03	0.0004 \pm 0.0008	0.005	31 \pm 20.5	100	51
DBSCAN ($\epsilon = 1$)	0.005 \pm 0.018	0.12	0.018 \pm 0.069	0.492	23 \pm 16	60	82
DBSCAN ($\epsilon = 1.5$)	0.478 \pm 0.112	0.9	0.0225 \pm 0.212	0.907	20 \pm 15	56	42
DBSCAN ($\epsilon = 2$)	0.412 \pm 0.348	0.99	0.55 \pm 0.35	0.996	7 \pm 7.5	34	10
k-means ($k = n$)	0.376 \pm 0.203	0.846	0.429 \pm 0.214	0.863	7 \pm 2.5	10	4
k-means ($k = n + 1$)	0.320 \pm 0.183	0.758	0.369 \pm 0.203	0.774	8 \pm 2.5	11	3
k-means ($k = n - 1$)	0.431 \pm 0.210	0.88	0.491 \pm 0.219	0.892	6 \pm 2.5	9	4
k-means ($k = 2n$)	0.129 \pm 0.130	0.43	0.166 \pm 0.175	0.524	14 \pm 5	20	38
k-means ($k = 4n$)	0.019 \pm 0.045	0.136	0.029 \pm 0.06	0.208	28 \pm 10	40	71
k-means ($k = 6n$)	4.1e-05 \pm 0.0002	0.001	2.24e-05 \pm 0.0001	0.0006	42 \pm 15	60	90
k-means ($k = 8n$)	2.1e-05 \pm 0.0001	0.0006	1.854e-05 \pm 9.4e-05	0.0006	55 \pm 19	80	90
OPTICS	0.003 \pm 0.0008	0.004	0.106 \pm 0.03	0.259	270 \pm 35	336	3
mean shift ($bw = \alpha$)	0.871 \pm 0.253	0.998	0.881 \pm 0.239	0.998	1.3 \pm 1.3	9	5
mean shift ($bw = \alpha/2$)	0.001 \pm 0.006	0.045	0.002 \pm 0.008	0.058	24 \pm 15	60	85
mean shift ($bw = \alpha/4$)	8.07e-06 \pm 7.7e-05	0.0007	1.5e-05 \pm 0.0001	0.001	25 \pm 15	62	93
mean shift ($bw = \alpha/8$)	0	0	0	0	36 \pm 28	152	94

to those of [17] and they indicate that RNNs learn non-minimal representations of regular languages.

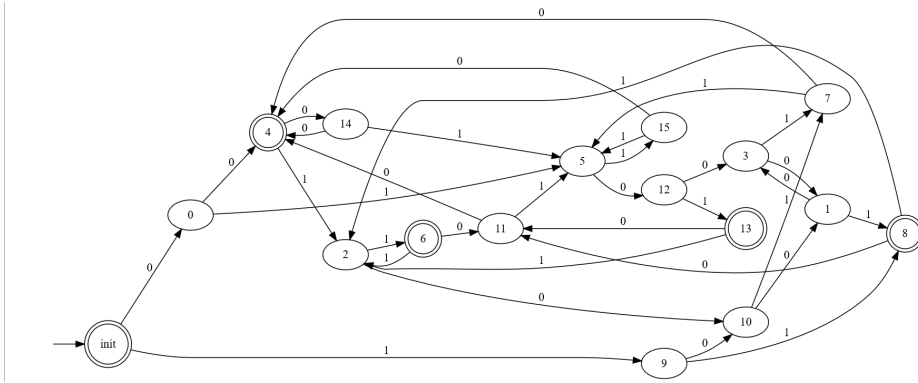


Fig. 9: Extracted cluster automata from an RNN trained on the Tomita 5 grammar. K-means clustering with $k = 4n$ was used. The extracted model is a non-minimal representation of the ground truth model shown in Fig. 9.